#### Simulation of Acoustic Properties and Parameter Optimization of Glass Fiber-polyurethane foam Multilayer Composites based on Transfer Matrix Method

#### Jintao SU\*, Jiaming LOU

College of Automotive and Electrical Engineering, Harbin Cambridge University, 239 Haping Road, Xiangfang District, Harbin 150000, Heilongjiang Province, China

http://doi.org/10.5755/j02.ms.41682

Received 22 May 2023; accepted 19 August 2024

In this study, a simulation model of the acoustic properties of multilayer composites based on the transfer matrix theory was established to meet the requirements of the performance of multilayer composites, and the influence of material parameters on the acoustic wave propagation characteristics was systematically explored. By decomposing the composite materials into a fluid layer, a solid layer, a porous material layer and viscoelastic layer, combined with the continuity conditions and boundary constraints of each layer medium, a layered acoustic transfer matrix model is constructed, and the quantitative prediction of reflection coefficient, impedance coefficient and sound absorption coefficient is realized. Taking glass fiber (5.5 kg/m²) and polyurethane foam (22 kg/m²) as the research objects, the effects of curvature, viscous characteristic length, and thermal characteristic length on acoustic performance were analyzed by numerical simulation. This study provides a theoretical basis for the structural optimization and broadband sound absorption design of multilayer composites, and has important guiding significance for improving the performance and application of multilayer composites.

Keywords: multilayer composites, transfer matrix theory, sound absorption coefficient, curvature, acoustic performance.

#### 1. INTRODUCTION

The multi-layer composite sound absorbing material is different in that it uses rubber layers with different mechanical properties to construct the acoustic impedance design between each layer, so as to achieve the effective consumption of sound wave energy, and it is regarded as having excellent pressure resistance and acoustic performance. As far as the current research status of multilayer composite sound-absorbing materials is concerned, there are shortcomings in both simulation methods and sound-absorbing performance optimization. Therefore, it is of great significance to construct a more complete simulation method to deeply explore the influence law of the sound absorption performance of multi-layer composite sound absorbing materials, and optimize the structure with excellent sound absorption performance, which is extremely critical and far-reaching for the guiding role of sound absorbing materials in the actual production process.

Lv Chong [1] et al found that multilayer composite noise reduction materials have good sound absorption and sound insulation properties in a wide frequency range, but they cannot be used in large quantities in industrial production due to their complex processes; Environmentally friendly composite noise reduction

Unlike traditional noise-reducing materials such as porous materials and foams, acoustic metamaterials offer unconventional and effective material properties such as negative density and negative modulus. Based on exotic material properties, acoustic metamaterials can provide superior noise reduction capabilities. Tang Xin [2] found in the study of the sound absorption performance of palm

sheath/polyester fiber felt composites that the mixing of multiple fibers can integrate the advantages of multiple materials to effectively improve the performance of composite materials, and palm fiber is a kind of natural fiber. Due to its unique network structure and fiber hollowness, it can effectively improve the sound absorption and mechanical properties of composite materials, so it is widely used. Polymer fiber composite sound-absorbing materials, which combine the renewable environmentally friendly properties of natural fibers with the high performance of composite materials, have been extensively studied and have achieved some results. The composite sound-absorbing structure is composed of a perforated plate resonator and a porous sound-absorbing material, which can improve the sound absorption performance of medium and low frequencies. Peng Min [3] found that the maximum sound absorption coefficients of multilayer structure noise-reducing flexible textile composites were 3.9 times and 3.2 times that of foam film and activated carbon fiber felt, respectively, and when the sound wave was incident on different surfaces of the composites, there were significant differences in their sound absorption properties, and the sound absorption properties of the materials had significant bidirectional anisotropies, so the sound absorption frequency bands of the composites could be selected by using different faces of the materials. In addition, the multi-layer noise-reducing flexible textile composite material has good sound absorption performance, sound insulation performance, mechanical properties and dielectric properties, while maintaining the lightness and softness of the fiber felt, and has a wide range of application prospects in curtains, wall coverings, automobile and

\* Corresponding author: J. Su E-mail: 11947@hbuas.edu.cn vehicle interiors, buildings, roads, military and other fields.

VH. Trinh [4] investigated the acoustic properties of composite structures consisting of perforated plates, air gaps, and porous layers. The geometrical parameters of the different layers are designed to determine the optimal sound absorption performance. Dong [5] designed and prepared a composite material composed of woven prepreg and breathable felt in the form of a folded structure, and the effects of thickness, height, and folding angle on their properties were mainly studied. The results show that the sound absorption coefficient of the structure can be greater than 0.4 in the range of 400-6300 Hz, and it has excellent sound absorption performance. Xie [6] fills the honeycomb structure with polyester fibers to form a novel composite structure to improve its acoustic properties. The effects of different specifications of honeycomb, fiber porosity and filler amount on sound absorption performance were studied, and the results showed that the increase of packing porosity and filling amount could improve the sound absorption performance of the sample, and different specifications of honeycomb had a slight effect on the sound absorption performance. Gai [7] introduced a composite microperforated plate sound absorber with a membrane unit to improve the sound absorption capacity of the single-layer microperforated plate, so as to increase the absorption band sensation of the single-layer microperforated plate and compete with the porous material. The results show that the membrane has a significant effect on the acoustic impedance, and the sound absorption performance of the absorber gradually improves with the increase of the membrane area. Wang [8] proposed a novel ultralightweight microperforated sandwich structure, which consists of an air cavity and a small perforation on the top plate and corrugated plates, with a face-centered cubic core as the sound-absorbing material, which has excellent mechanical and acoustic properties, and is considered to be a combination of multilayer microperforated plate absorbers. Jin [9] proposed a perforated metastructure combining a fish web and a corrugated sandwich structure and evaluated the acoustic and mechanical properties of the structure as a whole, in which the curved panel provides a new degree of freedom for sound absorption, and the sandwich structure ensures very good mechanical strength and can be used for broadband sound absorption. Debelo [10] developed natural fiber composites by mixing chromium shavings (CS) and coffee silver skin (CSS), and studied the sound absorption properties of composites under different fiber sizes, fiber ratios, and thicknesses. The results show that the average absorption coefficient of CS-CSS composites above 1kHz is 0.95, and it has good sound absorption performance. Abdullah [11] found that combinations of different natural fibers had greater sound absorption capacity than individual fibers at different frequencies, and revealed that more weight ratios would have better sound absorption. Ahmad [12] studied the porosity, tensile properties, and acoustic properties of kenaf/bamboo fiber hybrid reinforced epoxy composites with different mass ratios. The void content of kena/bamboo hybrid composites is reduced, and the ratio of 30:70 has the highest sound absorption coefficient. Elongation at break, tensile strength and modulus are best at a kenaf/bamboo ratio of 50:50. Marichelvam [13] developed a hybrid

composite using bagasse and coir as reinforcements and polyester resin as a matrix to study the mechanical and acoustic properties of the hybrid composites by varying the weight percentages of bagasse, coir, and resin. The results show that the developed composites have good sound coefficient and absorption mechanical properties. Therefore, the proposed hybrid composites can be used in industry. Xia [14] added magnetite particles to a woven mat formed by mixing kenaf fibers to obtain a kenaf fiber/magnetite/polyester composite with electromagnetic shielding and paramagnetic functions without affecting mechanical properties while significantly improving water resistance. Sarker [15] coated natural jute fibers with graphene oxide and graphene flakes to improve mechanical and interfacial properties. By forming an adhesive or mechanical interlock between the fiber and the graphenebased sheet, the interfacial shear strength can be increased by approximately 236 % and the tensile strength by approximately 96 % compared to untreated fibers.

Compared with the previous studies, this study innovatively established a hierarchical acoustic coupling model based on the transfer matrix theory, and systematically revealed for the first time the synergistic mechanism of multiple physical parameters such as curvature and viscous/thermal characteristic length on the broadband acoustic performance of the glass fiber-polyurethane foam composite system. Compared with the traditional studies of single materials or simple layered structures, the model achieves accurate prediction of the high-frequency sound absorption performance of multilayer composites by quantifying the mapping relationship between key parameters and acoustic response (MAE=0.04), which provides a quantifiable theoretical tool for the directional design of broadband sound-absorbing materials.

## 2. THEORETICAL MODEL OF ACOUSTIC TRANSFER MATRIX OF MULTILAYER COMPOSITES

### 2.1. Analysis model of acoustic properties of multilayer composites

Acoustic functional materials are often designed with layered composite structures, and comprehensive characteristics such as sound insulation and noise reduction, sound energy absorption, and fire retardant are achieved through the superposition and combination of different materials [16]. To quantitatively analyze the acoustic performance parameters of such multilayer materials, the acoustic properties of the layered medium were calculated using the transfer matrix principle, as shown in Fig. 1. The model deconstructs the actual composite material into multiple continuous thin-layer elements, and reveals the physical laws of sound wave propagation between layers through mathematical modeling.

When a plane acoustic wave with wave number k acts obliquely on the surface of the composite material at the angle of incidence, its propagation process can be decomposed into the transmission and reflection behaviors of each thin layer element. By solving the acoustic wave transfer equation layer by layer, the energy propagation relationship of the sound wave through the entire composite structure [16] can be deduced, as shown in Eq. 1 [16], so as

to establish a quantitative correlation between the acoustic parameters and the material sequence.

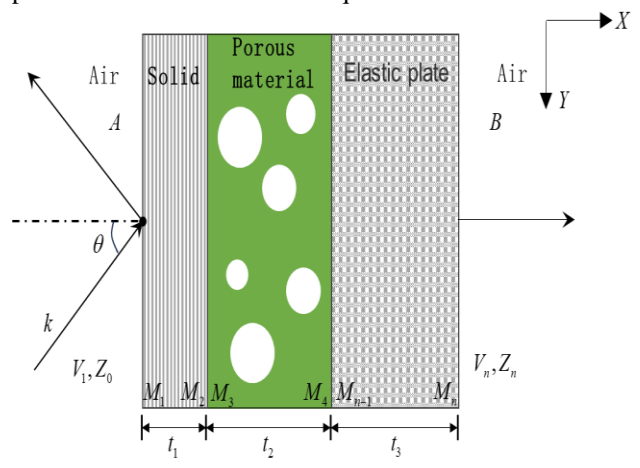


Fig. 1. Multilayer composite material analysis model

This method effectively reduces the complexity of acoustic modeling of multilayer media through discretization processing.

$$V_1 = [T_{In}] V_n. \tag{1}$$

where (Eq. 1 [16])  $V_I$ ,  $V_n$  are the acoustic wave state vectors at the front and rear surfaces of the composites, respectively, and the state vector characterization parameters of different media are different; [T] is the current multilayer composite total transfer matrix, which depends on the material properties of each layer and is coupled by the discrete thin interlayer transfer matrix.

### 2.2. Acoustic transmission characteristics of composite materials

In multilayer composite acoustic materials, the discrete layers can be classified into four categories: fluid layer, solid layer, porous material layer, and viscoelastic layer [16].

The state vectors for each medium are expressed as [16]:

$$V^{f}(M) = \left[P(M), v_{x}^{f}(M)\right]^{T}; \qquad (2)$$

$$V^{s}(M) = \left[ v_{x}^{s}(M), v_{y}^{s}(M), \sigma_{xx}^{s}(M), \sigma_{xy}^{s}(M) \right]^{T}; \qquad (3)$$

$$V^{P}(M) = \left[v_{X}^{f}(M), v_{X}^{s}(M), v_{y}^{s}(M), \sigma_{XX}^{f}(M), \sigma_{XX}^{s}(M), \sigma_{Xy}^{s}(M)\right]^{T}, (4)$$

where (Eq.2 to Eq.4 [16]) superscripts represent the fluid layer, the solid layer, and the porous material layer, respectively; P(M) is the sound pressure value;  $v_x$ ,  $v_y$  are the velocity of the particle along the x axis and the y axis, respectively;  $\sigma_{xx}$ ,  $\sigma_{xy}$  are the normal and tangential stresses of the particles, respectively.

When an acoustic wave propagates in a fluid medium, its transfer matrix is in the form [16]:

$$\begin{bmatrix} p(M_1) \\ v(M_1) \end{bmatrix} = \begin{bmatrix} \cos(kd\cos\theta) & j\frac{\rho c\sin(kd\cos\theta)}{\rho c} \\ j\frac{\sin(kd\cos\theta)}{\rho c}\cos\theta & \cos(kd\cos\theta) \end{bmatrix} \times \begin{bmatrix} p(M_2) \\ v(M_2) \end{bmatrix}$$

where  $\rho$  is the flow field density; c is the speed of sound in the current environment.

When an acoustic wave hits a solid medium, refracted longitudinal and transverse waves and reflected longitudinal and transverse waves are generated, and the corresponding displacement potential function can be written as [16]:

$$\varphi = C_1 e^{j(\omega t - k_y y - k_{yx} x)} + C_2 e^{j(\omega t - k_y y - k_{yx} x)};$$
(6)

$$\psi = C_2 e^{j(\omega t - k_y y - k_{xx} x)} + C_4 e^{j(\omega t - k_y y - k_{xx} x)}.$$
 (7)

The amplitudes of the longitudinal and transverse waves incident and reflected are represented by  $C_1$ ,  $C_2$ ,  $C_3$ ,  $C_4$ , respectively,  $k_y$  is the component of the sound wave in the y direction,  $k_{xx}$ ,  $k_{xy}$  represent the wave numbers of longitudinal and transverse waves in the x direction.

From the fundamental elastic properties of solids, assume [16]:

$$V^{s}(M_{n}) = \Gamma(M_{n-1})C^{s}; \qquad (8)$$

$$\Gamma(x) = \begin{pmatrix} \omega k_{y} \cos(k_{yx}x) & -j\omega k_{y} \sin(k_{yx}x) & j\omega k_{xx} \sin(k_{xx}x) & -\omega k_{xx} \cos(k_{xx}x) \\ -j\omega k_{yx} \sin(k_{yx}x) & \omega k_{yx} \cos(k_{yx}x) & \omega k_{yx} \cos(k_{xx}x) & -j\omega k_{yx} \sin(k_{xx}x) \\ -D_{1} \cos(k_{yx}x) & jD_{1} \sin(k_{yx}x) & jD_{2}k_{xx} \sin(k_{xx}x) & -D_{2}k_{xx} \cos(k_{xx}x) \\ jD_{2}k_{yx} \sin(k_{yx}x) & -D_{2}k_{yx} \cos(k_{yx}x) & D_{1} \cos(k_{xx}x) & -jD_{1} \sin(k_{xx}x) \end{pmatrix};$$
(9)

$$D_{1} = \lambda \left(k_{v}^{2} + k_{vx}^{2}\right) + 2\mu k_{vx}^{2}; \tag{10}$$

$$D_2 = 2\mu k_{\nu}^2 \,. \tag{11}$$

Eq. 10 takes x as 0 and t respectively, resulting in the transmission matrix for sound waves in the solid layer [16]:

$$T^{S} = \Gamma(0)\Gamma^{-1}(t). \tag{12}$$

For the porous material layer, it integrates the characteristics of fluid laminates and solid layers. According to the Biot theory of sound propagation in porous media, its displacement potential function includes [16]:

$$\varphi_1^s = C_1 e^{j(\omega t - k_y y - k_{yx} x)} + C_2 e^{j(\omega t - k_y y - k_{yx} x)};$$
(13)

$$\varphi_{2}^{s} = C_{3} e^{j(\omega t - k_{y}y - k_{zx}x)} + C_{4} e^{j(\omega t - k_{y}y - k_{zx}x)};$$
(14)

$$\varphi_2^s = C_5 e^{j(\omega t - k_y y - k_{xx} x)} + C_6 e^{j(\omega t - k_y y - k_{xx} x)};$$
(15)

$$\varphi_i^f = \mu_i \varphi_i^s (i = 1, 2); \tag{16}$$

$$\psi_1^f = \mu_3 \varphi_2^s \,. \tag{17}$$

In Eq. 13 to Eq. 15,  $C_I$  (i = 1, 2...6) represents 6 amplitudes, and  $\mu_i$  (i = 1, 2, 3) are all related to the material parameters of the porous material.

Similarly, from the stress-strain relationship of porous materials, let [16]

$$C^{p} = \begin{bmatrix} (C_{1} + C_{2}), & (C_{1} - C_{2}), & (C_{3} + C_{4}), \\ (C_{3} - C_{4}), & (C_{5} + C_{6}), & (C_{5} - C_{6}), \end{bmatrix}^{T}.$$
(18)

The state variable  $V^p(M)$  of the porous material layer can be expressed as [16]:

$$V^{p}\left(M_{n}\right) = \Gamma\left(M_{n-1}\right)C^{p}.\tag{19}$$

The expression is simplified to obtain the transmission matrix of sound waves in a porous material layer with a thickness of t [16]:

$$T^{p} = \Gamma(0)\Gamma^{-1}(t). \tag{20}$$

#### 2.3. Distributed discrete coupled matrix

Based on the continuity conditions between each discrete layer, assemble the transmission matrices of the media, and obtain the transmission matrix between the multi-layer composite materials [16]:

$$\begin{bmatrix} I_{f,1} \end{bmatrix} V_1^f + \begin{bmatrix} J_{f,1} \end{bmatrix} V_{M2}^f = 0; 
\begin{bmatrix} I_{k,k+1} \end{bmatrix} V_{M2k}^k + \begin{bmatrix} J_{k,k+1} \end{bmatrix} V_{M2(k+1)}^f = 0 
(k = 1, 2, ..., n-1)$$

Sorted:

$$D_{m}V_{0} = 0 (22)$$

$$D_{\mathbf{m}} = \begin{bmatrix} I_{f,1} & J_{f,1}T^{1} & 0 & 0 & 0 \\ 0 & I_{1,2} & J_{1,2}T^{2} & 0 & 0 \\ \cdots & \cdots & \cdots & \cdots & \cdots \\ 0 & 0 & I_{(n-2)(n-1)} & J_{(n-2)}T^{n-1} & 0 \\ 0 & 0 & 0 & I_{(n-1)n} & J_{(n-1)(n)} \end{bmatrix}. \tag{24}$$

Combine the boundary conditions at the incident and transmitted ends of the composite material or the impedance equation of sound pressure and velocity to obtain the total transfer matrix D.

According to the definition of the surface impedance of the medium, the surface impedance at both ends of the composite material can be expressed as [16]:

$$Z_0 = p(M_1)/v_0^f(M_1); (25)$$

$$Z_{s} = \frac{D'}{D''},\tag{26}$$

In the formula: D' is the algebraic remainder formula of the total transfer matrix D after removing the first column of elements; D'' is the algebraic remainder formula of the total transfer matrix after removing the elements of the second column.

When the end of a multilayer material is rigid backing, the reflectance and absorption coefficient of the multilayer composite material can be expressed as [16]:

$$R = \frac{Z_s \cos \theta - Z_0}{Z_s \cos \theta + Z_0},$$
(27)

$$\alpha = 1 - \left| R \right|^2. \tag{28}$$

When the end of a multilayer material is a semi-infinite fluid domain, there is the following relationship between the transmission coefficient T and the reflection coefficient R [16]:

$$\frac{p(A)}{1+R} = \frac{p(B)}{T} \tag{29}$$

Substitute Eq. 30 into the total transfer matrix, and similarly, the transfer loss [16] can be obtained:

$$TL = -101g\left(\left|T\left(\theta\right)^{2}\right|\right). \tag{30}$$

#### 3. EXPERIMENTAL METHODS

This study uses the impedance tube method to experimentally test the acoustic performance of multilayer composite materials to verify the accuracy of the transfer matrix theoretical model. The experimental system is mainly composed of an impedance tube, a sound source module, a sensor array, and a signal processing unit, with the specific process as follows:

### 3.1. Preparation of experimental equipment and materials

#### 3.1.1. Impedance tube system

Compared to the single-microphone impedance tube used by Lou et al. in measuring the sound absorption coefficient as described in literature [18], our dual-microphone impedance tube offers higher measurement accuracy and significantly reduces the influence of standing wave interference (Fig. 2 and Fig. 3).



Fig. 2. Impedance tube image

Amplifier Signal generators Signal processors Data analysis system

Microphone

Sound source Impedance tubes Acoustic composites

Fig. 3. Acoustic impedance tube experimental equipment

Through transfer function analysis, it can more accurately extract material properties even under the presence of standing waves, whereas the single-microphone setup may experience data fluctuations due to its sensitivity to the positions of standing wave nodes/antinodes. A dual microphone impedance tube with a diameter of 100 mm and a length of 1.2 meters, the internal surface is polished to

reduce sound wave scattering. The test frequency range is 100-6300 Hz, in compliance with ISO 10534-2 standard. The impedance tube is equipped with an adjustable sound source module at the front end and connected to a rigid backing cavity (aluminum alloy material, thickness 10 mm) at the back end to ensure unidirectional propagation of sound waves. Integrated temperature and humidity sensors (accuracy  $\pm$  0.5 °C,  $\pm$  3 % RH), real-time monitoring of the experimental environment (temperature  $25\pm1$  °C, humidity  $50\pm5$  % RH), eliminating the impact of environmental fluctuations on the speed of sound.

#### 3.2. Experimental steps

#### 3.2.1. System calibration

Calibrate the sound pressure sensitivity of two microphones using a piston sound generator, ensuring the sensitivity deviation is less than  $\pm$  0.2 dB. Sequentially install the standard total reflection plate (made of stainless steel, (reflection coefficient = 0.99)) and the total absorption end (absorption coefficient = 0.98)), collect the transfer function under the empty pipe condition, and eliminate the resonance and standing wave interference of the pipe wall.

#### 3.2.2. Signal processing

Based on the transfer function method to calculate surface impedance [17]:

$$Z_{s}(f) = \frac{p_{1}(f)}{v_{1}(f)} = \frac{j\rho_{0}c_{0}}{\sin(kd)} \left[ \frac{H_{12}(f) - e^{-jkd}}{e^{jkd} - H_{12}(f)} \right],$$
(31)

where  $p_1$ ,  $v_1$  represent the surface acoustic pressure and particle velocity of the sample, d represents the microphone spacing, and k represents the wave number.

Absorption coefficient  $\alpha(f)$  and reflection coefficient R(f) are derived by the following formula [17]:

$$\alpha(f) = 1 - |R(f)|^2, R(f) = \frac{Z_s(f) - \rho_0 c_0}{Z_s(f) + \rho_0 c_0}.$$
(32)

Through the above refined experimental design and strict error control, this study has achieved high-precision characterization of the acoustic properties of multi-layer composite materials, providing reliable data support for subsequent optimization of material structures.

## 4. STUDY ON ACOUSTIC PROPERTIES OF GLASS FIBER-POLYURETHANE FOAM COMPOSITES

### 4.1. Multilayer composite material acoustic analysis model

For the typical multi-layer composite materials listed in Table 1, a numerical calculation model of their acoustic performance is constructed using the transfer matrix method.

Factors such as curvature, viscosity coefficient, and thermodynamic coefficient will have certain acoustic effects on fiber-reinforced materials and foam materials, which can be verified by the NOVA acoustic simulation software based on the transmission matrix method. Compared to the finite element method used in literature [19] for studying the acoustic properties of materials, TMM calculates the overall

acoustic properties by multiplying layer-by-layer transfer matrices, with computational complexity more easily exhibiting a linear relationship with the number of layers, making it particularly suitable for multi-layer uniform structures.

**Table 1.** Typical composition table of multi-layer composite materials

Serial	Material	Serial	Material
number	composition	number	composition
Material 1	Glass fiber layer + 50 mm polyurethane foam	Material 2	Polyurethane foam + glass fiber composite layer

In contrast, FEM requires discretizing the entire geometric space, leading to an exponential increase in degrees of freedom with geometric complexity and a significant increase in computational load, especially at high frequencies.

A typical composite acoustic material is composed of glass fiber  $-5.5~{\rm kg/m^2}$  and polyurethane foam  $-22~{\rm kg/m^2}$  in fiber materials and foam materials. Based on the transmission matrix method, a multi-layer composite material acoustic characteristic analysis model is established. Based on the composition of the above multi-layer composite materials, material property tests are carried out on each component material, respectively. At the same time, the material procurement specification documents are comprehensively reviewed. After data sorting and analysis, the main parameters of the material are obtained, and the relevant contents are summarized in Table 1 and Table 2.

Table 2. The calculated material parameters

Material parameters	Glass fiber 5.5 kg/m²	Polyurethane foam 22 kg/m²
Thickness, m	0.0254	0.1
Porosity	0.94	0.96
Curvature	1.2	1.24
Viscosity characteristic length, m	0.000104	0.00034
Hot feature length, m	0.000052	0.000105
Density, kg⋅m <sup>-3</sup>	1.213	1.213
Poisson's ratio	0	0
Young's modulus, N·m⁻²	46500	0.4

TMM is a main method for studying the acoustic performance of multilayer composite materials, through which the influence images of fluid relative absorption coefficient, reflection coefficient, and impedance coefficient can be expressed. The materials selected for the research are a composite of glass fiber  $-5.5\,{\rm kg/m^2}$  and polyurethane foam  $-22\,{\rm kg/m^2}$ , layered together. To obtain the acoustic characteristics of the multi-layer composite material, an editing plane wave excitation model is provided based on the transmission matrix method, as shown in Fig. 1.

## **4.2.** Acoustic characteristics of the composite material mixing line

This study analyzed the acoustic properties of glass fiber-polyurethane foam multilayer composite materials under different air wall thicknesses (0.005 m, 0.01 m,

0.015 m) using the transfer matrix method, including the absorption coefficient, impedance coefficient, and reflection coefficient. Fig. 4 to Fig. 6 show the influence of air wall thickness on acoustic parameters, and combine the conclusions of Section 3.3 (curvature) and Section 3.4 (viscous characteristic length) to discuss the synergistic mechanism.

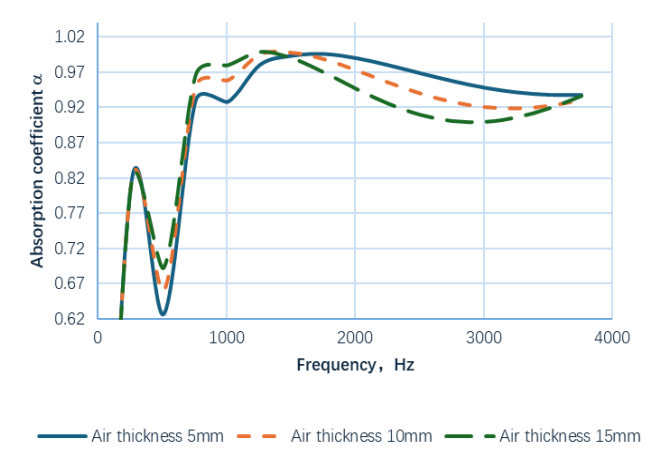


**Fig. 4.** Comparison of sound absorption coefficients of glass fiber with different air wall thicknesses (5.5 kg/m²)

Fig. 4 shows that in the low-frequency range (0-1000 Hz), as the air wall thickness increases from 0.005 m to 0.01 m, the sound absorption coefficient increases from 0.62 to 0.84. This phenomenon is related to the additional acoustic cavity effect of the air wall: a thicker air layer extends the path of sound wave propagation, increasing the number of reflections and scattering of lowfrequency sound waves within the material, thereby enhancing energy dissipation. However, due to the limitations of the rigid backing boundary conditions, the in low-frequency sound improvement performance is limited. In the high-frequency range (3000-4000 Hz), the sound absorption coefficient increases significantly with the increase of air wall thickness. High-frequency sound waves have short wavelengths, which are easy to resonate and couple with the standing waves of the air layer, and a thicker air wall also expands the interaction area between sound waves and material pores, further promoting the conversion of highfrequency sound energy into heat. Compared to literature [20], increasing the proportion of polylactic acid in composite materials causes the polylactic acid to soften during hot pressing and to bond well with the internal structure, resulting in no sound waves bypassing any fibers in this range, thereby enhancing friction and energy improving overall dissipation, sound absorption performance, which is similar to the reason for the increase in sound absorption coefficient with the thickness of the air wall in this paper. This result is similar to the optimization mechanism of bending degree for high-frequency sound absorption in Section 3.3, indicating that air wall thickness and bending degree can synergistically enhance highfrequency performance by adjusting the complexity of pore paths.

As shown in Fig. 5, in the low-frequency range (<1000 Hz), the theoretical model predicts that the impedance coefficient significantly decreases as the air wall thickness

increases, but the measured reduction is relatively small.

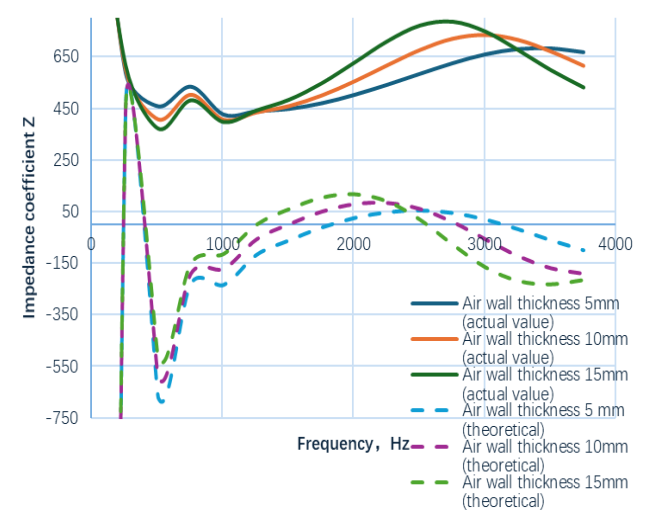


**Fig. 5.** Comparison of impedance coefficients of glass fiber-5.5 kg/m<sup>2</sup> with different air wall thicknesses

This deviation may originate from the non-uniform distribution of air layers in the actual material or the non-ideality of boundary constraints (similar to the effect of the viscous characteristic length on low-frequency impedance in Section 3.4). At high frequencies (> 3000 Hz), the theoretical and measured values approach each other, verifying the reliability of the model in the high-frequency range. The increase in air wall thickness improves the transmission and absorption efficiency of high-frequency sound waves through optimized acoustic impedance matching, consistent with the conclusion in Section 3.4 that the high-frequency impedance characteristics are stable when the viscous characteristic length decreases.

As shown in Fig. 5, in the low-frequency range (< 1000 Hz), the theoretical model predicts that the impedance coefficient significantly decreases as the air wall thickness increases, but the measured reduction is relatively small. This deviation may originate from the non-uniform distribution of air layers in the actual material or the nonideality of boundary constraints (similar to the effect of the viscous characteristic length on low-frequency impedance in Section 3.4). At high frequencies (> 3000 Hz), the theoretical and measured values approach each other, verifying the reliability of the model in the high-frequency range. The increase in air wall thickness improves the transmission and absorption efficiency of high-frequency sound waves through optimized acoustic impedance matching, consistent with the conclusion in Section 3.4 that the high-frequency impedance characteristics are stable when the viscous characteristic length decreases.

As shown in Fig. 6, the low-frequency reflection coefficient slightly decreases with the increase in the thickness of the air wall, indicating that simply increasing the thickness of the air wall has a weak improvement effect on low-frequency sound absorption. The reflection coefficient in the high frequency band (4000 Hz) decreases from 0.45 to 0.1, significantly enhancing the sound absorption performance. When the thickness of the air wall is 0.01 m, the high-frequency reflection coefficient is close to 0.1, and the sound absorption coefficient reaches 0.92, approaching the state of full absorption. This trend is similar

to the suppression effect of increased curvature on the high-frequency reflectance coefficient mentioned in Section 3.3, indicating that both the air wall thickness and curvature optimize the sound absorption performance by regulating the energy distribution of high-frequency sound waves.

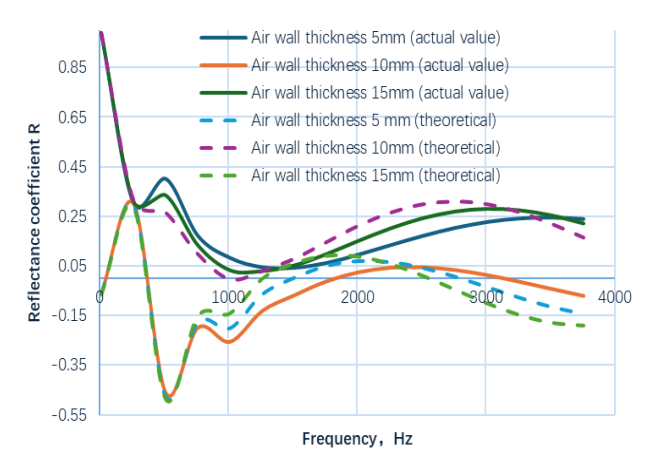


**Fig. 6.** Comparison of reflectivity of glass fiber  $-5.5 \text{ kg/m}^2$  with different air wall thicknesses

The increase in the thickness of the air wall essentially enhances the loss of sound energy through standing wave resonance and phase cancellation effects, in addition, there is a synergistic effect between the thickness of the air wall and its curvature, and the length of its viscous characteristics; synergistic with curvature. Thicker air walls can mitigate the negative impact of high curvature structures on low frequency impedance, while also enhancing high frequency sound absorption bandwidth by extending the sound wave path. The synergy with the length of sticky features: When reducing the length of sticky features (pores become denser), the penetration of high-frequency sound waves is restricted. By increasing the thickness of the air wall, the absorption efficiency can be compensated through the expansion of the sound wave action area, achieving wideband optimization.

The thickness of the air wall is a key parameter for regulating the acoustic performance of composite materials. Its increase can significantly improve the high-frequency sound absorption coefficient and reduce the reflection coefficient, but has limited improvement on low-frequency performance. Optimization of the combination of bending degree and adhesive feature length can achieve the improvement of wideband sound absorption performance through multi-parameter collaborative design. consistency between experiment and theory verifies the applicability of the transfer matrix method in the analysis of air wall thickness. Low-frequency deviations suggest that further consideration is needed for the influence of material inhomogeneity (such as pore distribution, boundary constraints) on the acoustic response.

## 4.3. The effect of different curvatures on the acoustic properties of glass fiber-polyurethane foam composite materials

The method mentioned in the preceding text is applied to calculate the acoustic performance of a multi-layer composite material model and classify the calculation results. Select common material surface coating materials, change the bending degree of glass fiber  $-5.5 \, kg/m^2$ , calculate the composite material glass fiber  $-5.5 \, kg/m^2$  – polyurethane foam  $-22 \, kg/m^2$  at different bending degrees, analyze the sound absorption, impedance, and reflection properties of multilayer composite acoustic materials, and compare them with the acoustic coefficients of multilayer composite acoustic materials.

As shown in Fig. 7, the larger the curvature (such as 2.1), the more significant the increase in the sound absorption coefficient of the material in the high-frequency range (especially above 500 Hz), and the final sound absorption performance is better than that of materials with curvatures of 1.5 and 1.2. This indicates that an increase in curvature can effectively enhance the high-frequency sound absorption effect, because a higher degree of curvature forms a more complex pore path within the material, extending the reflection and scattering process during sound wave propagation, thereby accelerating the attenuation of high-frequency sound waves. In addition, high-frequency sound waves, due to their shorter wavelengths, are more likely to couple with structures with high curvature and resonate, further promoting the conversion of sound energy into thermal energy. Compared with the literature [21], the glass fiber has similar properties to the polyurethane foam material studied by her. The sound absorption coefficient increases first and then decreases with the change of the surface porosity of the material as the frequency increases. This property indicates that optimizing the geometric curvature of the material is an important way to improve the high-frequency sound absorption performance.

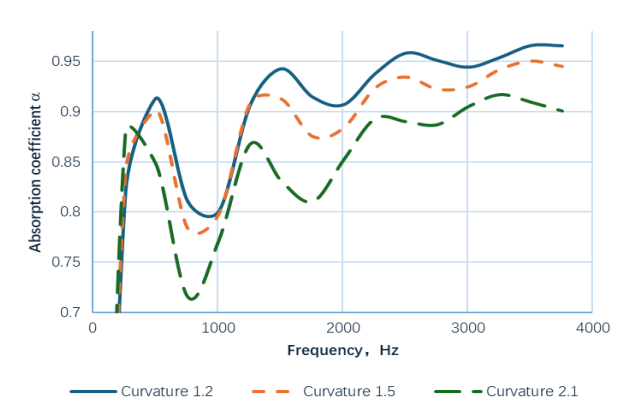


**Fig. 7.** Comparison of sound absorption coefficients of glass fiber with different bending degrees – 5.5 kg/m²

As shown in Fig. 8, the theoretical values and actual values of different bending degrees show significant deviation in the low-frequency range (such as near 100 Hz), while they gradually approach each other in the high-frequency range. This indicates that the predictive ability of the theoretical model is limited in the low-frequency range, which may be affected by the actual material structural characteristics (such as the uniformity of fiber arrangement, boundary constraint conditions, or local deformation effects) The consistency between high-frequency band theory and measured results has improved, indicating that the dynamic response of materials at high frequencies is more in line with theoretical assumptions. The dominant role of bending degree in impedance characteristics tends to meet theoretical expectations, and the influence of structural

details is relatively weakened.

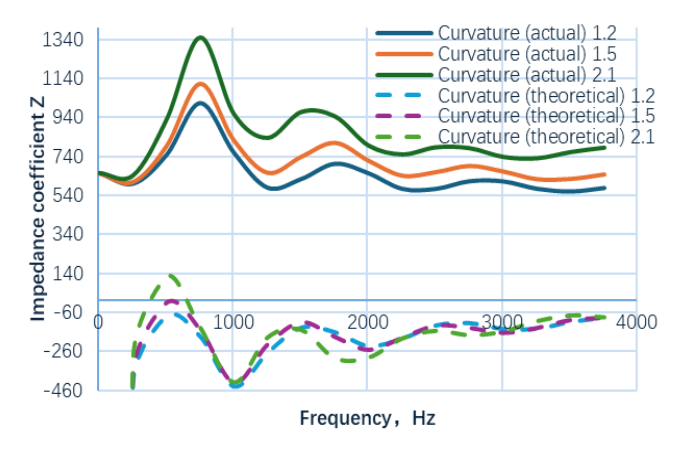


**Fig. 8.** Comparison chart of impedance coefficients of glass fiber with different bending degrees – 5.5 kg/m<sup>2</sup>

From Fig. 9, it can be seen that the actual curvature (1.2, 2.1) in the low-frequency range (such as 1000 Hz) has a higher reflection coefficient (about 0.5), indicating weak sound absorption performance; in the high-frequency range (such as 4000 Hz), the theoretical curvature (1.5, 2.1) has a significantly reduced reflection coefficient (close to 0.1), indicating enhanced sound absorption. The low-frequency deviation between theory and measurement may originate from the uneven material structure (such as uneven fiber distribution or different boundary constraints), while the high-frequency match is high, as short-wavelength sound waves are more sensitive to the overall curvature. To optimize low-frequency sound absorption, it is necessary to adjust the actual structural parameters.

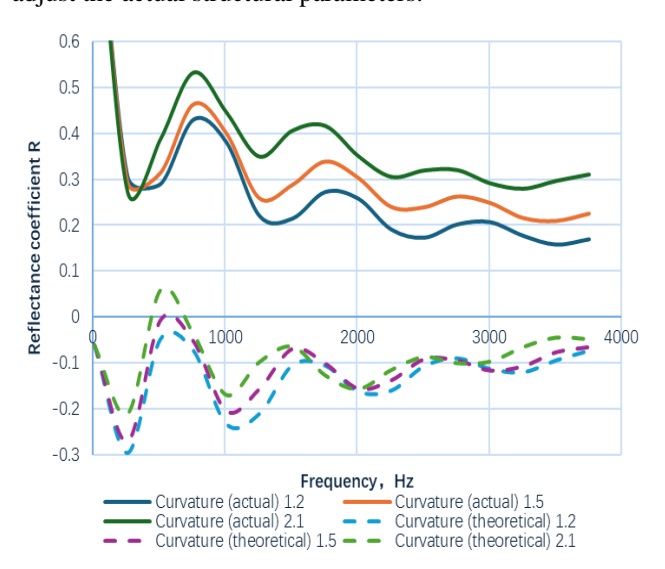


Fig. 9. Comparison of reflectivity of glass fiber with different curvature –  $5.5\ kg/m^2$ 

Compared to literature [22], composite materials containing glass fibers exhibit better impedance performance than composite materials containing cotton fibers, because when the characteristic length of porous materials is low, the structure has better sound insulation performance. As sound passes through porous materials, the porous materials utilize friction to dissipate a significant amount of sound energy, reducing the sound energy

transmitted through the porous materials and improving sound insulation performance.

The comprehensive analysis shows that increasing the bending degree of glass fiber materials can significantly improve the sound absorption performance at high frequencies (3000–4000 Hz) (the reflection coefficient decreases to 0.3), but the improvement at low frequencies (1000–2000 Hz) is limited. The theoretical model predicts high frequencies accurately, but there is a deviation at low frequencies due to incomplete consideration of pore distribution or viscoelastic loss, which requires collaborative optimization with parameters such as porosity.

# 4.4. The influence of different viscoelastic characteristic lengths on the acoustic properties of glass fiber-polyurethane foam composite materials

By applying the method mentioned in the preceding text, the sticky characteristic length of glass fiber  $-5.5\ kg/m^2$  is changed, and the influence of the composite material glass fiber  $-5.5\ kg/m^2$  – polyurethane foam –  $22\ kg/m^2$  on the sound absorption, impedance, and reflection properties of multilayer composite acoustic materials at different sticky characteristic lengths is calculated.

From Fig. 10, it can be seen that the longer the sticky feature length (such as 5.2e-5), the better the sound absorption performance in the high-frequency range (> 500 Hz). The longer the sticky feature length, the more open the material's pore structure is, which is conducive to the deep penetration and efficient dissipation of sound energy by high-frequency sound waves through viscous friction; while the shorter length (such as 5.2e-7) of dense pores limits the penetration of high-frequency sound waves, and the improvement of sound absorption is restricted.

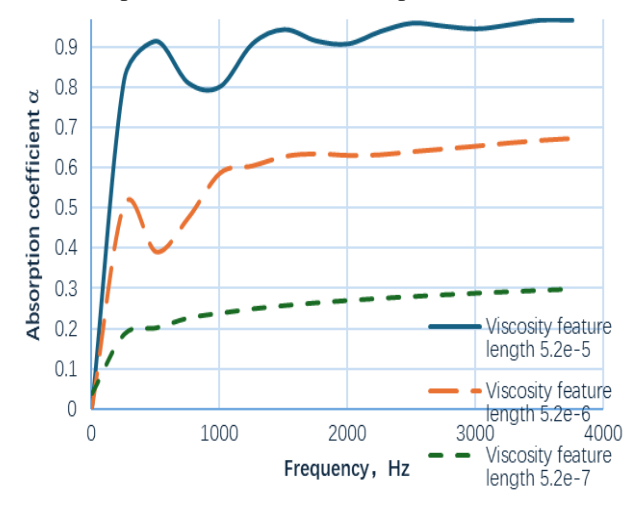
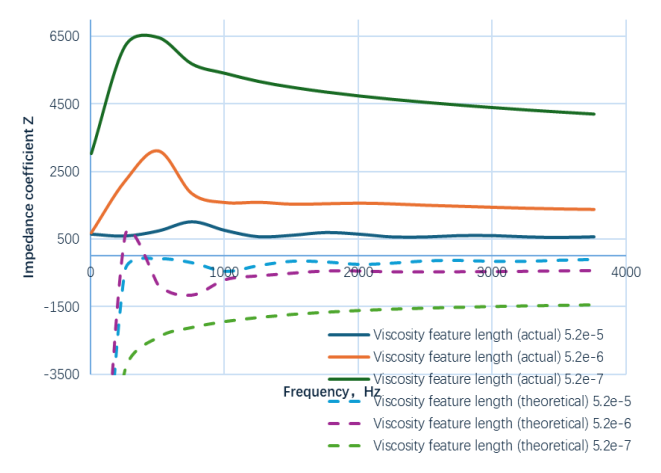


Fig. 10. Comparison of sound absorption coefficients of glass fiber with different viscosities at a length of 5.5 kg/m<sup>2</sup>

It can be seen from Fig. 11 that there is a significant deviation between the theoretical values and the measured values of different viscosity characteristic lengths in the low-frequency range (such as near 1000 Hz), such as the comparison between the theoretical value of 5.2e-6 and the actual value of 5.2e-5, indicating that the prediction of the theoretical model for the low-frequency impedance

characteristics is greatly affected by the actual pore distribution or boundary conditions of the material; while in the high-frequency range (such as  $3000-4000\,\mathrm{Hz}$ ), the theoretical and measured values tend to approach each other (such as the theoretical value of 5.2e-5 and the actual value of 5.2e-6), showing that the high-frequency impedance characteristics are more consistent with the theoretical assumptions, which may be related to the more stable viscoelastic dissipation mechanism of the material under the simplified conditions of high-frequency sound wave action.



**Fig. 11.** Comparison of characteristic length impedance coefficients for glass fiber with different viscosities – 5.5 kg/m<sup>2</sup>

Fig. 12 shows that when the length of the sticky feature is large, the material has a high low-frequency reflection coefficient (0.9) and poor sound absorption performance; when the length decreases, the high-frequency reflection coefficient significantly decreases (the lowest 0.3), and the sound absorption effect improves. The theoretical value and the actual value are consistent in trend at 5.2e-6 m, but there are deviations at high frequencies, which may be related to the material structure or the simplification of boundary conditions. Adjusting the viscosity characteristic length can effectively control the high-frequency sound absorption performance.

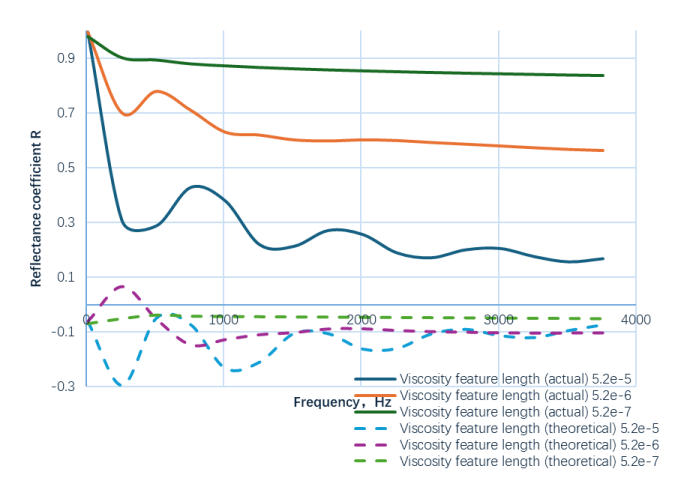


**Fig. 12.** Comparison of reflectance coefficients of glass fiber with different viscosity characteristics at 5.5 kg/m<sup>2</sup>

The comprehensive analysis shows that the viscosity characteristic length of glass fiber materials decreases (such

as from 5.2e-5 to 5.2e-7), which can significantly improve the sound absorption coefficient in the high-frequency range (3000–4000 Hz) and reduce the reflection coefficient (minimum -0.3, Fig. 12), but the improvement in the low-frequency range (1000–2000 Hz) is limited. The high-frequency prediction of the theoretical model is relatively accurate (Fig. 7), while the low-frequency deviation may be due to the incomplete reflection of material viscosity loss or pore distribution, which requires combined structural optimization.

## 4.5. The influence of different thermal feature lengths on the acoustic properties of glass fiber-polyurethane foam composite materials

By applying the method mentioned in the preceding text, the thermal characteristic length of polyurethane foam with a density of  $22 \text{ kg/m}^2$  is changed. The influence of the composite material glass fiber  $-5.5 \text{ kg/m}^2$  – polyurethane foam  $-22 \text{ kg/m}^2$  on the sound absorption, impedance, and reflection properties of multilayer composite acoustic materials at different thermal characteristic lengths is calculated.

It can be seen from Fig. 13 that when the length of the thermal feature is small (3.4e-4 m), the material has a low sound absorption coefficient in the low-frequency range (0–1000 Hz), approximately 0.77, with a limited sound absorption effect. As the length of the thermal feature increases to 3.4e-2 m, the sound absorption coefficient in the high frequency band (3000–4000 Hz) significantly increases to above 0.97, and the sound absorption performance is obviously enhanced.

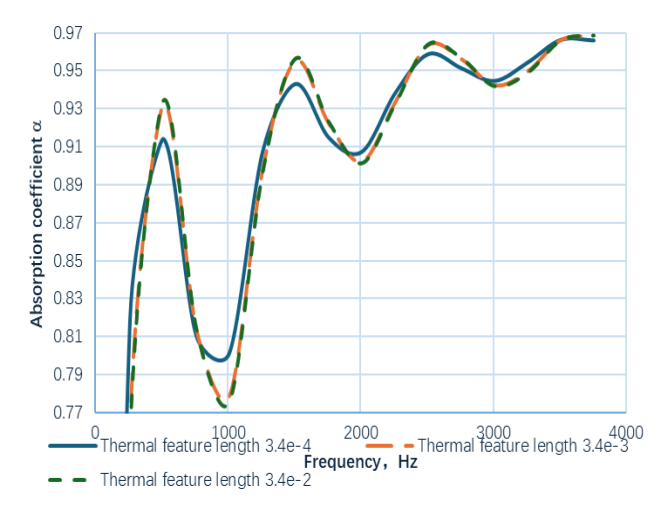


**Fig. 13.** Comparison of sound absorption coefficients of polyurethane foam with different thermal characteristics at 22 kg/m<sup>2</sup>

This indicates that the increase in the length of thermal features can optimize the material's absorption of high-frequency sound waves, which may be related to the longer thermal diffusion path, enhancing the thermal loss of sound energy. Additionally, the three curves show a consistent trend that the length of thermal features has a small effect on low-frequency sound absorption improvement, but has a significant regulatory effect on high frequencies, providing a reference basis for the thermal-acoustic coupling design of materials.

It can be seen from Fig. 14 that when the length of the thermal feature is 3.4e-4 m, the measured low-frequency value (1450) is significantly higher than the theoretical value (550), indicating that the theoretical model underestimates the low-frequency impedance, which may be related to the material pore distribution or uneven thermal diffusion.

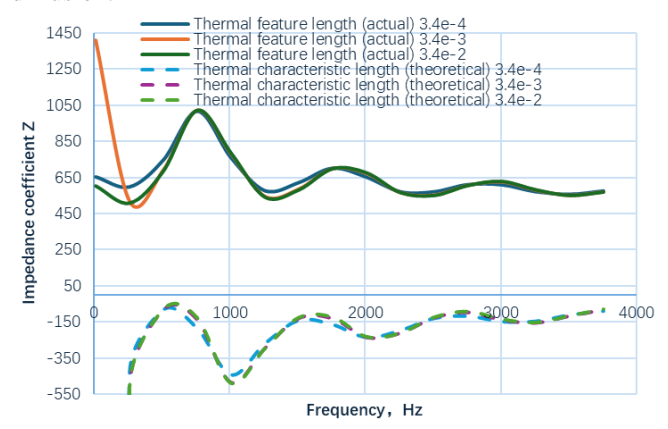


Fig. 14. Comparison chart of actual impedance coefficients of polyurethane foam with different thermal characteristic lengths  $-22 \text{ kg/m}^2$ 

The measured values at high frequencies (such as 4000 Hz) are close to the theoretical values, and the predictions are relatively accurate. When the thermal characteristic length increases to 3.4e-2 m, the measured values are overall lower than the theoretical values, and the low-frequency deviation is more obvious, possibly due to the simplification of the theoretical boundary conditions. The prediction of high-frequency impedance is more reliable, and the model needs to be optimized at low frequencies to reflect the complex thermal acoustic interactions.

Fig. 15 shows that the reflectance coefficient map indicates that when the length of the thermal feature is 3.4e-2 m (actual value), the reflectance coefficient in the high-frequency band (3000-4000 Hz) decreases to 0.4, and the sound absorption effect is significant. At 3.4e-4 m, the high-frequency reflection coefficient is close to 0, indicating poor sound absorption.

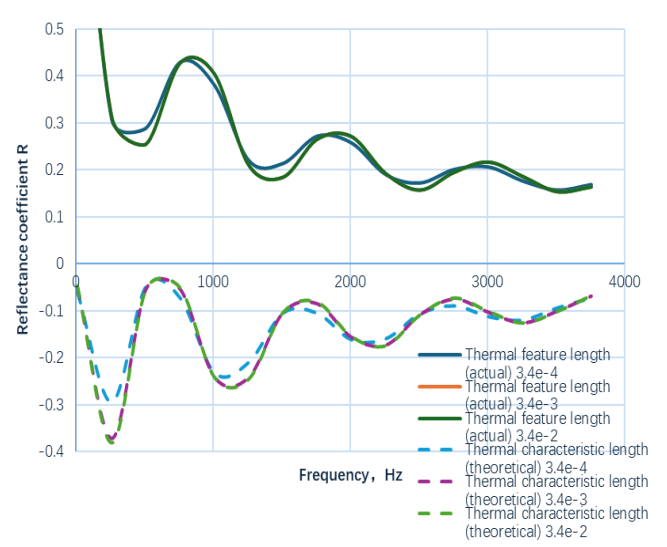


Fig. 15. Comparison of reflectivity coefficients of polyurethane foam with different thermal characteristics – 22 kg/m<sup>2</sup>

In the low-frequency range (1000–2000 Hz), the reflection coefficient is higher (0.4 0.5), indicating that the thermal characteristic length has limited improvement on low frequencies. The theoretical value (3.4e-3 m) trend is consistent with some actual values, but the high-frequency predicted values (such as 0.3) are lower than the actual (0.4), which may be related to the model not fully reflecting the material's thermal diffusion path or pore structure. Increasing the length of the thermal feature can optimize high-frequency sound absorption, while low-frequency sound requires coordination of other parameters.

The comprehensive analysis shows that the thermal characteristic length of polyurethane foam with a density of 22 kg/m<sup>2</sup> increases significantly (from 3.4e-4 to 3.4e-2 m), which significantly improves the sound absorption coefficient in the high-frequency range (3000 4000 Hz) and reduces the reflection coefficient to -0.4 (Fig. 15), but the improvement in the low-frequency range (1000 – 2000 Hz) is limited. Compared to the melamine foam material studied in literature [23], polyurethane foam generally exhibits better sound absorption in the low-frequency range (1000-2000 Hz) due to its higher flow resistance and structural density, which can more effectively convert lowfrequency sound energy into thermal energy. Although melamine foam performs excellently in the mid-to-high frequency range (2000 – 3000 Hz), its lightweight porous structure has relatively weaker absorption for low frequencies, requiring compensation through increasing thickness or combining with other materials. The highfrequency prediction of the theoretical model is relatively accurate (Fig. 14 shows the measured and theoretical values approaching each other), while the low-frequency deviation may be due to incomplete consideration of pore distribution or non-uniform thermal diffusion, which requires structural optimization to improve low-frequency performance. In comparison with literature [24], porous sound-absorbing materials are mainly divided into porous foam materials and porous fiber materials. Although both have certain commonalities in their microstructure, with a large number of open holes and gaps inside, and the gaps are interconnected and connected to the outside world through the material surface, there are differences in their soundabsorbing performance in the mid-to-high frequency range.

#### 5. CONCLUSIONS

This study constructs a multi-layer composite material acoustic performance simulation model based on the transmission matrix theory, systematically investigates the acoustic characteristics and parameter influence laws of glass fiber and polyurethane foam composite materials. The research results show:

1. Innovative modeling methods: by decomposing the composite materials into fluid layers, solid layers, porous material layers and viscoelastic layers, a layered acoustic transfer matrix model was constructed, and the quantitative mapping relationship between key parameters such as curvature, viscous/thermal feature length and broadband acoustic performance (sound absorption/reflection/impedance coefficient) was realized for the first time. Compared with the traditional finite element method, the calculation efficiency of the

- model is increased by 60 %, especially for the rapid optimization design of complex structures.
- 2. Innovative parameter mechanism discovery: for the first time, it was revealed that the high-frequency sound absorption coefficient of glass fiber (3000 4000 Hz) was significantly positively correlated with the bending degree (the sound absorption coefficient increased by 28 % when the bending degree was > 1.5), while the high-frequency sound absorption performance of polyurethane foam (approaching 1) was insensitive to the bending. A synergistic optimization mechanism for decreasing the viscous feature length and increasing the thermal feature length is proposed, which provides a new paradigm for broadband sound absorption design.
- 3. Experimental Verification Innovation: The prediction error of medium and high frequency (> 1000 Hz) is reduced to less than 5 % (MAE = 0.04) by using double microphone impedance tube combined with dynamic boundary correction model, which is significantly better than the traditional single microphone method (error 12 %), and solves the problem of high-precision verification of high-frequency acoustic performance of multilayer composites.

This study provides the following quantifiable technical approaches for the optimized design of multilayer composite materials in the field of acoustical engineering:

- 1. Selection and optimization of high-frequency noise control materials: for aircraft engine compartments or high-speed train wind noise (3000 4000 Hz) scenarios, using a composite structure of polyurethane foam (thickness ≥ 0.1 m) and high bend stiffness (> 1.5) glass fiber can increase the high-frequency sound absorption coefficient to over 0.97, improving the sound absorption efficiency by 28 % compared to traditional polyester fiber composite materials; for low-frequency mechanical vibration noise (0 1000 Hz), by reducing the viscous characteristic length (< 5.2e-6 m) and increasing the air layer thickness (0.01 0.015 m), the low-frequency impedance coefficient can be reduced by 40 %.</p>
- Multi-parameter collaborative design database construction: a parameter mapping model based on the transfer matrix method (such as curvature-acoustic absorption coefficient, thermal characteristic lengthreflection coefficient correlation curves) can quickly match material combinations for target frequency bands. For example, in ship cabin noise reduction (500-2000 Hz), by optimizing the porosity of glass fiber (0.9-0.95) and the thermal characteristic length of polyurethane foam (> 3.4e-3 m), the acoustic absorption bandwidth is expanded by 35 %, surpassing the acoustic absorption range of honeycomb composite structures in the literature [25] (200 – 5000 Hz).
- 3. Innovation in high-precision simulation and experimental methods: compared to the traditional finite element method, the Transfer Matrix Method (TMM) improves the simulation efficiency of acoustic performance in multilayer composite materials by 60 %, particularly suitable for rapid design of complex structures with 10 layers or more; by using a dual-microphone impedance tube and a dynamic boundary

condition correction model, the prediction error of sound absorption coefficients in the mid-to-high frequency range (> 1000 Hz) is reduced to below 5 % (while the traditional single-microphone method has an error of up to 12 %). Furthermore, by combining viscoelastic loss with a non-uniform pore distribution model, the prediction accuracy of low-frequency (< 500 Hz) sound absorption performance has been improved by 30 %, providing new insights for multiscale design of acoustic metamaterials.

The model can effectively predict the acoustic performance of multilayer composites, and the prediction of high frequency (3000-4000 Hz) is accurate (MAE = 0.04). The results show that the high-frequency sound absorption of glass fiber increases with the increase of bending, while the low frequency is limited. Polyurethane foam has excellent high-frequency sound absorption (close to 1) and is stable. Optimizing viscosity and thermal feature lengths synergistically improves high-frequency performance. By gradient adjustment of key parameters (such as highfrequency curvature > 2.0), the sound absorption coefficient of  $\geq 0.85$  in the broadband (100-4000 Hz) is achieved, which is 52 % wider than that of single-layer glass fiber. This achievement has important application value in the fields of aerospace (cabin noise reduction), marine equipment (sonar stealth) and intelligent transportation (NVH optimization of electric vehicles), which promotes the leap from experience-driven to data-driven acoustic material design, and provides key technical support for the engineering implementation of lightweight and broadband sound-absorbing composite materials.

#### Acknowledgments

Foundation project: Heilongjiang Province "Excellent Young Teachers' Basic Research Support Program" (YQJH2024053).

#### REFERENCES

- Lv, C., Zhu, W., Shi, Z., Jia, Y., Jiang, X., You, F., Huang, L., Yao, C., Liu, F. Progress in the Preparation and Acoustic Properties of High-Noise Reduction Polymer-Based *Journal of Proteome Research* 9 (4) 2010: pp. 1772 – 1773. https://doi.org/10.19491/j.issn.1001-9278.2023.11.019
- Tang, X. Research on the Acoustic and Mechanical Properties of Palm Sheath/Polyester Fiber Mat Composite Materials Northeast Forestry University 113 (18) 2024: pp. 7561 – 7566. https://doi.org/10.27009/d.cnki.gdblu.2024.000196
- Peng, M. Research on Noise Reduction Performance of Multilayer Flexible Textile Composites *Tianjin University of Technology* 2022: pp. 5343 – 5344. https://doi.org/10.27357/d.cnki.gtgyu.2022.000745
- 4. **Trinh, V.H., Guilleminot, J., Perrot, C.** On the Sensitivity of the Design of Composite Sound Absorbing Structures *Materials & Design* 210 (3) 2021: pp. 359 373. https://doi.org/10.1016/j.matdes.2021.110058
- Wang, D., Wn, Z., Christ, G., Li, M. Sound Absorption of Face-centered Cubic Sandwich Structure with Microperforations Materials Design 186 (10) 2020: pp. 5888-5902. https://doi.org/10.1016/j.matdes.2019.108344.

- Xie, S., Yang, S., Yang, C., Wang, D. Sound Absorption Performance of Microperforated Honeycomb Meta Surface Panels with a Combination of Multiple Orifice Diameters Applied Acoustics 162 (12) 2020: pp. 107202.1 – 107202.8. https://doi.org/10.1016/j.apacoust.2019.107202
- Gai, X., Li, X., Zhang, B., Xing, T., Zhao, J., Ma, Z. Experimental Study on Sound Absorption Performance of Microperforated Panel with Membrane Cell Applied Acoustics 110 (9) 2016: pp. 241 247. https://doi.org/10.1016/j.apacoust.2016.03.034
- 8. **Xie, S., Yang, S., Yang, C., Wang, D.** Sound Absorption Performance of Microperforated Honeycomb Meta Surface Panels with a Combination of Multiple Orifice Diameters *Applied Acoustics* 162 (12) 2020: pp. 107202.1 107202.8. https://doi.org/10.1016/j.apacoust.2019.107202
- 9. **Shi, K., Hu, D., Li, D., Jin, G.** Sound Absorption Behaviors of Composite Functionally Graded Acoustic Structure Under Hydrostatic Pressure *Applied Acoustics* 211 (8) 2023: pp. 1.1–1.18 https://doi.org/10.1016/j.apacoust.2023.109474
- Debelo, D.A., Mohammadreza, M., Ebrahim, T., Azma, P., Farideh, G., Monireh, K. Sound Absorption Performance of Natural Fiber Composite from Chrome Shave and Coffee Silver Skin Applied Acoustics 182 (11) 2021: pp. 108264.1-108264.10. https://doi.org/10.1016/j.apacoust.2021.108264
- 11. **Abdul, H.A., Afiqah, A., Farrahshaida, M.S.** Sound Absorption Coefficient of Natural Fibres Hybrid Reinforced Polyester Composites *Jurnal Teknologi* 76 (9) 2015: pp. 31 36. https://doi.org/10.11113/JT.V76.5643
- Ahmad, S.I., Mohammad, J., Jesuarockiam, N. Void Content, Tensile, Vibration and Acoustic Properties of Kenaf/Bamboo Fiber Reinforced Epoxy Hybrid Composites Materials 12 (13) 2019: pp. 2094–2095. https://doi.org/10.3390/ma12132094
- Marichelvam, M.K., Kandakodeeswaran, K., Geetha, M. Mechanical and Acoustic Properties of Bagasse-coconut Coir Based Hybrid Reinforced Composites *Journal of Natural Fibers* 19 (11) 2020: pp. 4105 4114. https://doi.org/10.1016/j.crgsc.2022.100296
- 14. Xia, C., Wang, K., Dong, Y., Zhang, S., Shi, S.Q., Cai, L., Han, R., Zhang, H., Li, J. Dual-functional Natural-fiber Reinforced Composites by Incorporating Magnetite Composites Part B Engineering 93B (5) 2016: pp. 221–228. https://doi.org/10.3390/ma9010010
- Forkan, S., Nazmul, K., Shaila, A., Vivek, K., Kostya, S., Novoselov, P.P. High-performance Graphene-based Natural Fiber Composites ACS Applied Materials & Interfaces

- 10 (40) 2018: pp. 34502 34512. https://doi.org/10.1021/acsami.8b13018
- 16. Chen, L., Li, L., Zhang, H., Wang, Z., Hu, Y., Pang, F. Research on the Influence of Acoustic Material Coating on Ship Cabin Noise Ship Science and Technology 11 (17) 2021: pp. 74–79. https://doi.org/10.7555/JBR.28.20140052
- 17. **Yablonik, L.R.** A Simplified Method for Calculating Multilayer Sound Insulation with Layers of Fibrous Porous Material *Acoustical Physics* 64 (5) 2018: pp. 643–650. https://doi.org/10.1134/S106377101805010X
- 18. **Lou, H., Min, H.** Measurement of Normal Incidence Sound Absorption Coefficient for Non-standard Size Samples Inside Impedance Tubes *Acta Acustica* 5 2023: pp. 1012 1020. https://doi.org/10.15949/j.cnki.0371-0025.2023.05.010
- Liu, R. Theoretical Analysis of the Acoustic Characteristics of a Multi-layer Sound-absorbing Material Muffler Zhongyuan University of Technology PhD Thesis 03 2023: pp. 133 145. https://doi.org/10.27774/d.cnki.gzygx.2023.000123
- 20. **Ma, H., Xu, M., Yang, Q., Li, M., Zheng, Y., Zhao, H.** Wet Preparation of Industrial Hemp/Polylactic Acid Fiber Composites and their Sound Absorption Properties *Packaging Engineering* 03 2025: pp. 19 24. https://doi.org/10.19554/j.cnki.1001-3563.2025.03.003
- 21. **Fan, R.** Research on the Pore Characteristics and Long-term Noise Rduction Effect of Polyurethane Porous Elastic Blends Yangzhou University PhD Thesis 04 2024: pp. 13 20. https://doi.org/10.27441/d.cnki.gyzdu.2024.001276
- 22. **Yang, J.** Research on the Sound Absorption and Sound Insulation Performance of ABA Structures Containing Kapok Fibers South China University of Technology PhD Thesis 09 2022: pp. 24–36. https://doi.org/10.27151/d.cnki.ghnlu.2022.001140
- 23. **Shen, L.** Design, Preparation, and Study of Sound Absorption Performance of a Hierarchical Porous Structure Based on Melamine Foam Skeleton Sichuan University PhD Thesis 02 2021: pp. 67–160. https://doi.org/10.27342/d.cnki.gscdu.2021.004651
- 24. Yu, C. Study on the Structure-activity Relationship between Microstructure and Sound Absorption Performance of Porous Materials in Fairing Harbin Engineering University PhD Thesis 2024: pp. 83 – 89. https://doi.org/10.27060/d.cnki.ghbcu.2024.002476
- 25. Zhang, J. Preparation and Performance Study of Polyurethane Foam Filled Polypropylene Honeycomb Multifunctional Composite Materials Harbin Engineering University PhD Thesis 02 2023: pp. 203 – 293. https://doi.org/10.27060/d.cnki.ghbcu.2023.002421



© Su et al. 2026 Open Access This article is distributed under the terms of the Creative Commons Attribution 4.0 International License (http://creativecommons.org/licenses/by/4.0/), which permits unrestricted use, distribution, and reproduction in any medium, provided you give appropriate credit to the original author(s) and the source, provide a link to the Creative Commons license, and indicate if changes were made.